THE ASTROPHYSICAL JOURNAL, 247:894–907, 1981 August 1

THE INTERMEDIATE AGE GLOBULAR CLUSTER NGC 152 IN THE SMALL MAGELLANIC CLOUD

P. W. HODGE[1]
Astronomy Department, University of Washington
Received 1980 December 29; accepted 1981 February 17

ABSTRACT

The color-magnitude diagram of the populous Small Magellanic Cloud cluster NGC 152, measured to $V \approx 22$, shows that it has an age of about 8×10^8 years and is moderately metals-deficient. Its giant branch is sparsely populated, but includes at least two carbon stars at very red colors. There is a richly populated clump of intermediate-color giants at $M_V \approx 0$. Several superluminous giants are detected, also at intermediate colors, but averaging $M_V \approx -2.0$. The C-M diagram for the nearby field has very similar properties to those of the cluster.

Subject headings: clusters: globular — galaxies: Magellanic Clouds — stars: abundances — stars: evolution

I. INTRODUCTION

This paper is part of a series of studies of intermediate age "blue globular" clusters of the Magellanic Clouds. The series has as its goal the determination of the ages and other features of these clusters from color-magnitude diagram studies. The most interesting aspect is the shape and distribution of stars in the giant regions of the clusters, which form a unique resource for the study of stellar evolution because of the large numbers of giants present. Previous papers have dealt with clusters in the range of age from 5×10^7 to 10^8 years (Hodge 1963; Flower and Hodge 1975; Baird *et al.* 1974; Flower 1976; Flower *et al.* 1980). We have until now concentrated toward the younger end of this range, because of the availability of excellent and fairly complete stellar evolutionary models for such stellar masses. In this paper, however, we give the results for one of a number of older clusters on our program. Because of theoretical problems with the degeneracy that arises in models at $\sim 2\ M_{\odot}$, the comparison with theoretical evolutionary patterns in this case is less complete.

Gascoigne (1980) and Walker (1979 and several earlier references listed there) have both examined several members of the class of clusters sometimes called "anomalous Magellanic clusters." These are objects that originally appeared from early surveys (Gascoigne and Kron 1952; Hesser, Hartwick, and Ugarte 1976; Hodge 1960) to be bona fide globular clusters, but which were subsequently found to have colors (Searle, Wilkinson, and Bagnuolo 1980 and many previous references) that suggested differences from what are considered true globular clusters. The morphology of the giant branch also seemed anomalous in some of the earlier studies. Gascoigne (1980) and Walker (1971) were able to show that the objects in question are younger than true globular clusters by going to faint enough limits of photometry that the main sequences were detected. Absolute magnitudes at main sequence turnoff were found to be on the order of +1 for these objects, indicating an age of approximately 1 billion rather than 12 billion years.

NGC 152 in the Small Magellanic Cloud (SMC) is a particularly favorable cluster for this kind of study for two reasons: It is reasonably clear of the most crowded region of the Small Magellanic Cloud so that photometry can be carried to faint limits; second, its structure is sufficiently loose that a fairly complete census of its members can be made right up to the center of the cluster. Its color in the *UBV* system has been measured at $B-V = +0.70$ (Alcaino 1978) and $+0.67$ (van den Bergh and Hagen 1968), suggesting that its age is probably intermediate between the young and the true globular clusters.

II. OBSERVATIONS

The observational data on NGC 152 were obtained at the Cerro Tololo Inter-American Observatory in 1979 September and 1980 October–November. Plates (Table 1) were obtained at the prime focus of the CTIO 4 meter telescope. For all plates an auxiliary wedge (Pickering 1891; Racine 1969) 18 cm in diameter was placed in the telescope beam to form secondary images to extend the photometry beyond the photoelectric direct measurements. Plates of 47 Tucanae were taken in each color on each night to calibrate the difference in magnitudes between the primary and secondary images, and in all cases this difference was found to be 6.88 ± 0.03 mag.

Photoelectric measurements were made of 15 stars adjacent to NGC 152, ranging in magnitude from $V = 7.82$ to $V = 19.42$ and $B-V$ of -0.03 to $B-V$ of

[1] Visiting Astronomer, Cerro Tololo Inter-American Observatory, operated by AURA, Inc., under NSF contract AST 74-04129.

TABLE 1

PLATES OF NGC 152

Plate	Emulsion	Exposure (minutes)	Filter	Seeing (arcsec)
2260	IIa-D	30	GG495	2
2264	IIa-O	10	GG385	2–3
2265	IIa-O	30	GG385	2
2266	IIa-O	30	GG385	2–3
2282	IIa-D	2	GG495	3
2283	IIa-D	5	GG495	3
2287	IIa-D	10	GG495	3–4
2288	IIa-D	30	GG495	2
2289	IIa-D	30	GG495	2
4351	IIa-O	3	GG385	1.5
4352	IIa-O	30	GG385	1.5
4353	IIa-O	10	GG385	1.5
4354	IIa-O	2	GG385	1.5
4355	IIa-D	2	GG495	1.5

1.96. It was intended to carry-the photoelectric sequence to fainter magnitudes, but cloudy weather prevented this. However, with the use of the auxiliary prism, it was possible to extend the effective calibration to $V = 21.72$ and $B = 22.48$ (Table 2). The internal consistency of this extension was checked both for the 47 Tucanae plates and the plates of NGC 152 and is excellent, with a formal probable error of only 0.05 mag. The photoelectric magnitudes were determined directly by comparison at the telescope with equatorial *UBV* standards, and are therefore independent of any other sequences in the Magellanic Clouds.

III. DATA REDUCTIONS

Using a Cuffey iris astrophotometer, *all* stars that were reasonably well separated from their neighbors in NGC 152 were measured on the plates for which they were measurable. The stars are identified in Figure 1, and data are given in Table 3.

IV. THE PRELIMINARY COLOR-MAGNITUDE DIAGRAM

In Figure 2 we plot the magnitudes and colors of all measured stars in the area of NGC 152 designated in Figure 1. This figure includes both stars that are field stars and foreground stars, unrelated to NGC 152, as well as a very large number of stars for which the probable error as determined by comparison of magnitudes on various plates is large due to image crowding. We show it in order to give an idea of the distribution of stars in the color-magnitude diagram for a nearly complete cluster sample. The cluster contains a large number of stars on the main sequence and a concentration of stars in the giant region, in both cases involving approximately 3 times as many stars for the cluster as for the field (these statistics will be discussed in more detail below). It should be emphasized that the complete color-magnitude diagram shown in Figure 2 is populated with many points for stars that we, in our previous papers, would have excluded from the photometry because of crowding. For this complete sample, the probable errors are calculated to be on the average 0.08 for V and 0.19 for B. For the limited sample discussed in § VI below, however, the sampling was limited to those stars for which the probable error in $V \leq 0.07$.

V. FIELD STARS

Figure 3 shows the area of sky which was chosen for purposes of determining the nature of the foreground and background star population. It is located 5′ northeast of NGC 152 at a position where the SMC star density is very nearly equal to that at NGC 152. The area of the field chosen is equal to that of the star cluster field. All stars brighter than $V = 19.6$ in the field were measured with the astrophotometer, and for the indicated sector of the field a complete sample to $V = 21.8$ was measured (Table 4). The resulting color-magnitude diagram is shown in Figure 4. It resembles fairly closely the color-magnitude diagram of the cluster, a circumstance that has been found true in general in the Magellanic Clouds (e.g.,

TABLE 2

PHOTOELECTRIC SEQUENCE

Star	V	$B-V$	$U-B$	$S(V)$	$S(B-V)$	$S(U-B)$	n	V'	B'
A	12.72	0.54	−0.03	±0.01	±0.01	±0.01	8	19.60	20.14
B	14.51	0.99	−0.70	0.03	0.04	0.05	3	21.39	22.38
C	11.17	0.58	0.06	0.02	0.02	0.02	7	18.05	18.63
D	14.84	0.76	0.32	0.01	0.03	0.04	4	21.72	22.48
E	16.39	1.96	...	0.06	0.10	...	3	...	...
F	15.96	0.74	...	0.11	0.15	...	8	...	...
H	17.37	1.39	...	0.18	0.18	...	8	...	...
M	19.42	0.90	...	0.20	0.22	...	4	...	...
X	16.86	−0.03	...	0.09	0.10	...	5	...	...
Y	13.16	0.53	0.02	0.02	0.01	0.01	3	20.04	20.67
Z	13.51	0.65	0.13	0.07	0.01	0.01	3	20.39	21.04
AA	12.12	0.50	−0.02	0.02	0.01	0.02	3	19.00	19.50
CC	9.71	1.27	1.29	0.02	0.01	...	3	16.59	17.86
DD	7.82	0.90	0.61	...	...	...	1	14.70	15.60
VF	18.74	0.76	...	0.14	0.14	...	5	...	...

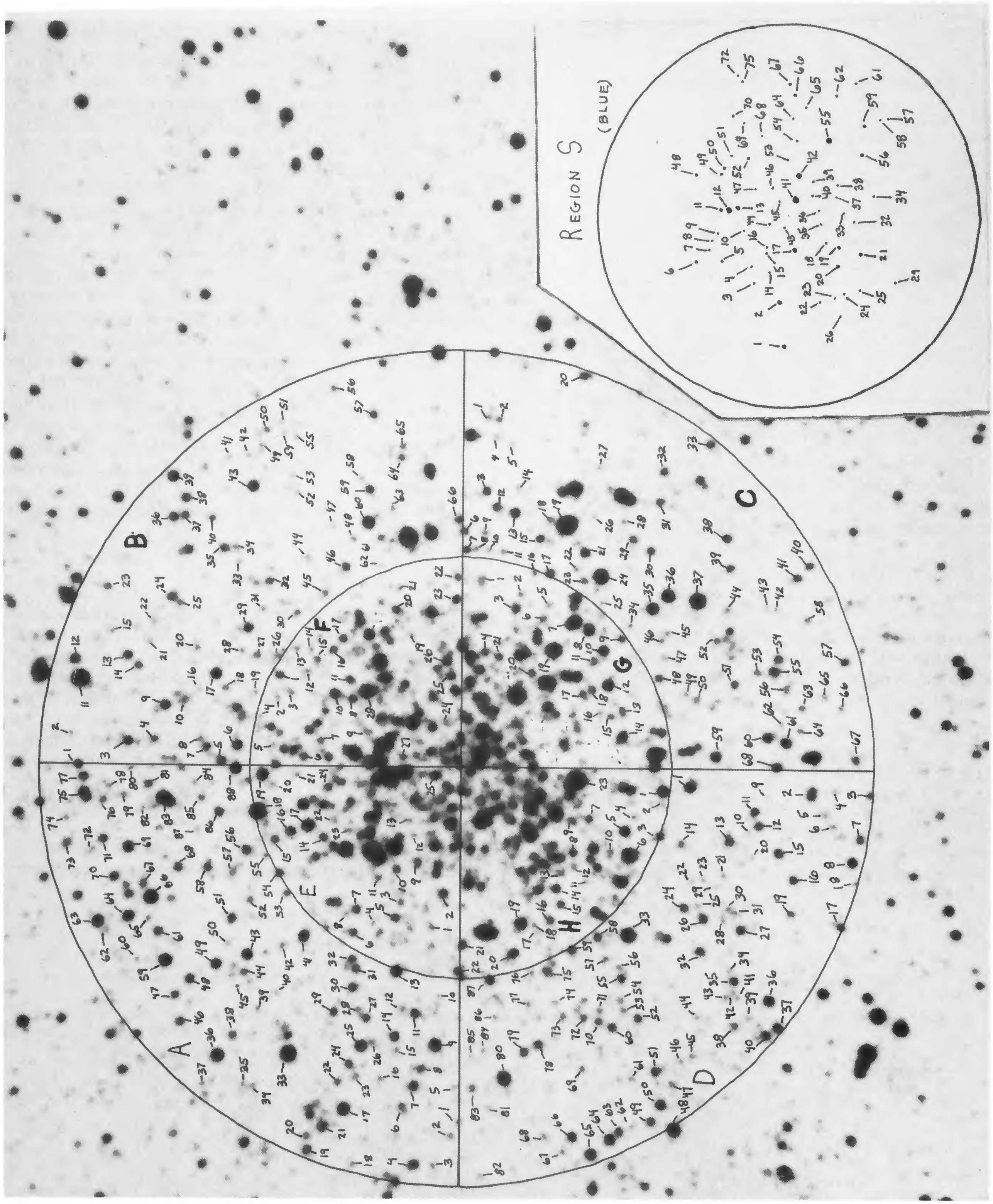

FIG. 1a

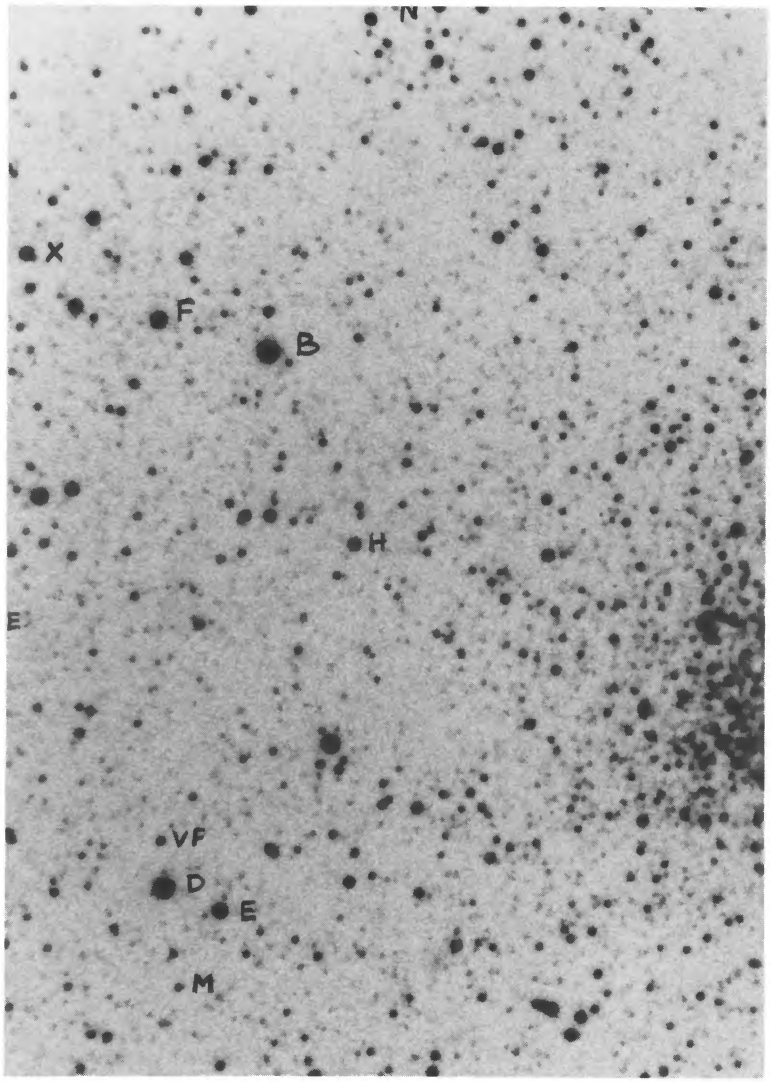

FIG. 1*b*

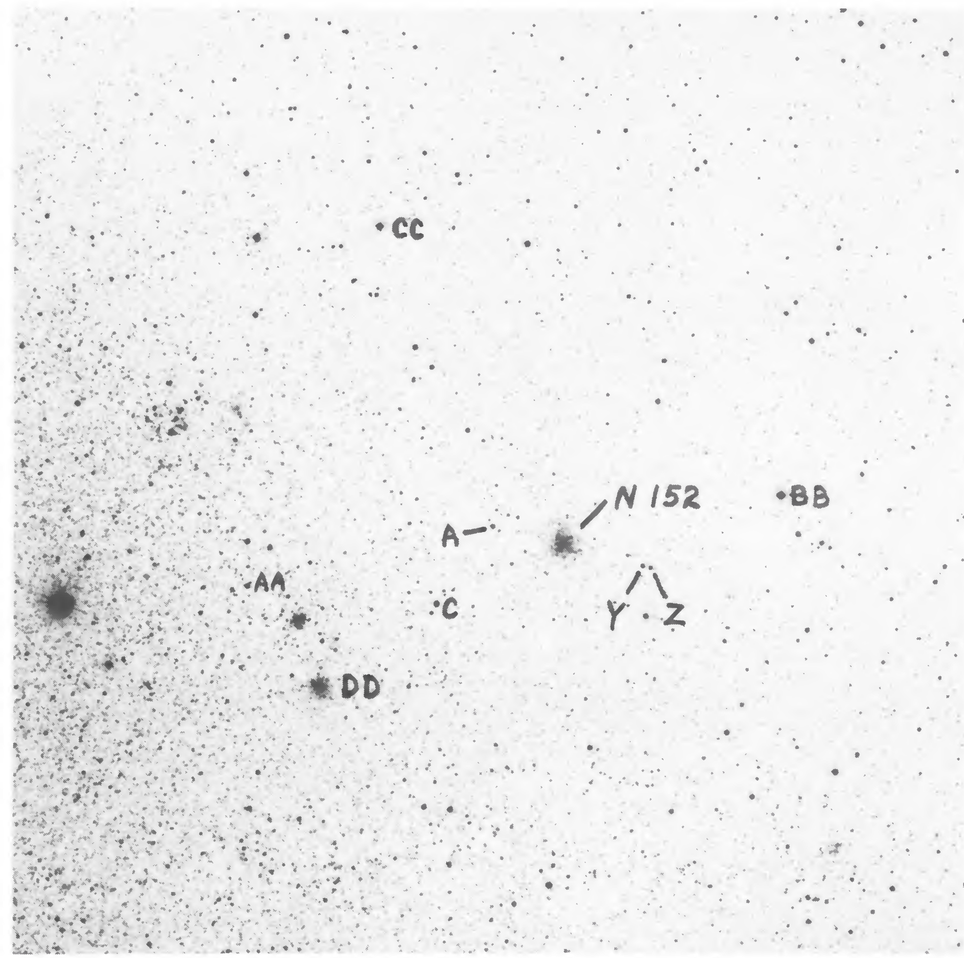

FIG. 1*c*

FIG 1.—(*a*) (*facing page*) NGC 152 from a CTIO 4 m plate in *V*. Measured stars are identified. The right insert shows the central stars. (*b*, *c*) (*this page*) show the more distant p.e. standards.

TABLE 3

PHOTOGRAPHIC MEASURES IN NGC 152

Star	V	$B-V$
A1	21.14	0.25
A2	21.16	−0.05
A3	21.21	0.00
A4	19.11	0.42
A5	21.64	0.05
A6	19.85	0.62
A7	18.97	0.81
A8	19.55	0.68
A9	18.06	1.17
A10	21.61	0.21
A11	19.07	0.84
A12	20.55	0.66
A13	18.23	1.02
A14	19.12	1.03
A15	21.04	−0.16
A16	21.08	−0.24
A17	18.14	1.27
A18	21.10	−0.42
A19	19.26	0.99
A20	20.46	0.77
A22	20.58	0.78
A23	20.44	−0.14
A24	19.56	0.75
A25	18.40	1.04
A26	20.34	−0.31
A27	19.44	0.72
A28	20.51	−0.06
A29	19.63	0.98
A30	19.19	0.85
A32	19.17	0.82
A33	17.11	1.57
A34	20.96	−0.31
A35	21.20	−0.36
A36	17.99	1.77
A37	21.27	−0.25
A39	21.25	0.07
A40	21.37	0.21
A41	18.41	0.90
A42	20.69	0.06
A43	18.60	1.17
A44	20.01	0.65
A46	19.58	0.93
A47	19.77	1.15
A48	19.34	1.00
A49	18.91	1.07
A50	21.48	0.25
A51	19.16	0.70
A52	20.50	0.60
A53	20.05	0.09
A54	19.31	0.78
A55	20.87	−0.13
A56	18.98	0.66
A58	19.15	0.85
A59	18.01	1.10
A60	21.53	−0.16
A61	19.32	0.95
A62	20.61	−0.14
A64	18.40	1.08
A65	21.01	0.06
A66	17.61	1.31
A67	19.43	0.10
A68	19.38	0.90
A69	18.54	1.16
A70	19.10	0.99
A71	19.39	0.84
A72	20.88	−0.07
A73	19.65	0.69
A74	21.00	0.12
A75	18.31	1.10
A76	19.93	0.79
A77	19.12	0.80
A78	20.74	−0.43
A79	20.66	−0.01
A80	20.98	0.13
A81	19.61	0.88
A82	21.17	−0.32
A84	21.27	−0.06
A85	20.36	0.03
A86	19.12	0.78
A87	21.35	0.09
A88	18.27	0.92
B1	19.21	1.10
B2	21.35	0.09
B4	19.98	−0.07
B5	19.01	0.67
B6	18.75	1.00
B7	19.13	0.84
B8	20.43	−0.24
B9	18.80	1.11
B10	18.94	1.26
B11	16.52	1.93
B12	18.89	0.98
B13	19.23	1.08
B14	19.72	1.10
B15	21.26	0.40
B16	21.36	−0.03
B17	18.35	1.14
B18	20.46	−0.24
B19	21.02	0.02
B20	20.53	0.49
B21	21.37	0.57
B22	21.14	−0.25
B23	20.11	0.83
B24	19.28	0.52
B26	19.97	0.06
B27	20.06	0.00
B28	21.04	−0.26
B29	18.82	1.03
B30	20.26	0.04
B31	20.93	−0.03
B32	19.65	0.92
B33	21.28	−0.53
B34	20.37	0.18
B35	19.39	0.76
B36	19.02	1.71
B37	19.39	0.93
B38	19.27	0.95
B40	20.19	1.00
B41	21.49	−0.18
B42	21.28	−0.01
B44	21.03	−0.15
B45	20.19	0.00
B46	19.23	0.78
B47	21.39	0.19
B48	20.71	0.07
B50	20.57	0.37
B51	21.46	−0.38
B52	21.35	0.10
B53	21.51	−0.05
B54	21.48	−0.62
B55	21.00	−0.42
B56	20.66	0.15
B57	19.42	1.03
B58	20.93	−0.08
B59	19.17	1.02
B60	17.85	1.31
B61	20.03	0.65
B62	21.36	−0.25
B63	20.96	0.09
B64	19.86	0.23
B65	20.29	0.56
B66	19.13	0.84
C1	20.47	0.23
C2	20.32	0.79
C3	19.26	0.66
C4	20.91	−0.02
C5	21.14	−0.11
C6	19.29	0.81
C7	19.33	0.80
C8	20.03	0.14
C9	20.50	0.32
C10	20.78	−0.49
C11	20.69	0.77
C12	19.18	0.99
C13	18.72	1.10
C14	21.10	0.42
C15	19.29	0.68
C16	20.51	−0.01
C17	19.01	0.80
C18	19.99	0.31
C19	15.88	1.71
C20	19.25	0.57
C21	18.88	0.81
C22	20.82	0.38
C23	19.85	0.05
C24	17.12	0.28
C25	21.05	0.28
C26	21.41	0.37
C27	21.13	0.43
C28	20.85	0.08
C29	19.41	0.88
C30	19.54	1.12
C31	19.45	1.00
C32	19.50	0.85
C33	19.41	0.83
C34	20.80	−0.17
C35	17.98	1.34
C36	17.75	1.21
C37	17.02	1.11
C38	19.23	0.92
C39	19.52	0.82
C40	19.74	1.23
C41	19.48	1.02
C42	21.22	−0.29
C43	21.31	−0.31
C44	20.57	0.10
C45	20.62	−0.15
C46	20.36	−0.21
C47	21.06	0.13
C48	19.53	0.96
C49	20.92	−0.49
C50	20.12	0.09
C51	19.51	0.98
C52	19.96	−0.08
C53	20.25	0.80
C54	19.31	0.67
C56	19.97	−0.14
C57	19.66	1.06
C58	20.82	0.72
C59	18.51	0.96
C60	18.69	0.84
C61	18.60	0.51
C62	21.10	−0.39
C63	20.34	0.09
C64	20.72	−0.03
C65	21.10	0.07
C66	21.10	0.37
C67	19.60	0.77
D1	18.29	0.82
D2	18.70	0.96

TABLE 3. (continued)

Star	V	B − V	Star	V	B − V	Star	V	B − V
D3	20.19	0.84	D87	18.83	0.89	H16	19.32	0.87
D4	21.22	0.24	E1	20.45	0.05	H18	20.74	−0.31
D6	20.91	0.36	E2	18.92	0.72	H19	17.94	1.09
D7	19.54	0.78	E3	20.17	0.17	H21	19.12	0.83
D8	18.92	0.99	E4	20.90	−0.33	H22	18.76	0.64
D9	21.79	0.21	E5	19.18	0.28	H23	15.98	1.66
D10	21.72	−0.34	E6	19.51	0.69	S1	16.90	1.19
D11	19.31	0.81	E7	19.31	0.93	S2	17.93	0.43
D12	19.34	0.76	E9	19.18	0.34	S3	19.15	0.54
D14	20.07	0.19	E10	19.39	1.09	S4	18.44	0.61
D15	19.18	0.94	E11	19.92	0.59	S5	16.84	3.17
D16	19.39	1.02	E12	20.86	−0.24	S6	17.32	0.17
D17	19.41	1.00	E13	20.52	−0.25	S7	18.25	0.66
D18	21.10	0.10	E14	19.11	0.92	S8	18.24	0.39
D19	20.34	0.81	E15	19.32	0.91	S9	19.05	0.39
D20	21.66	−0.13	E16	18.74	0.92	S10	18.86	0.10
D21	20.94	−0.11	E17	17.99	0.70	S11	17.73	0.88
D22	21.36	−0.40	E18	16.70	1.58	S12	16.21	0.93
D23	21.17	−0.06	E19	18.07	1.14	S13	17.35	0.87
D24	19.28	0.90	E21	20.86	−0.43	S14	18.95	0.60
D25	21.03	0.88	E22	20.27	0.07	S15	17.82	0.85
D26	19.18	0.82	E24	19.16	0.99	S16	18.84	0.46
D27	19.13	0.76	E25	18.48	0.61	S17	16.96	0.68
D28	20.76	−0.36	F1	19.42	0.75	S18	18.88	0.50
D29	21.48	−0.33	F2	20.77	−0.40	S19	17.58	0.66
D33	17.47	1.19	F3	20.36	−0.38	S20	17.28	0.42
D34	21.31	−0.37	F6	19.17	0.76	S21	17.19	0.70
D34	21.31	−0.37	F7	19.70	0.71	S22	19.07	0.31
D35	19.33	0.80	F8	18.83	1.05	S23	19.11	0.35
D36	18.68	1.19	F9	19.67	0.13	S24	18.60	0.68
D37	18.77	0.94	F10	18.57	0.98	S25	18.80	0.19
D38	20.12	0.87	F11	19.19	1.06	S26	18.90	0.75
D39	21.14	0.07	F12	20.37	−0.09	S29	18.76	0.82
D44	21.39	0.03	F13	20.52	−0.11	S32	18.99	0.61
D45	20.99	−0.08	F14	20.71	−0.26	S33	18.53	0.38
D46	21.44	−0.45	F15	19.97	0.04	S34	19.02	0.47
D47	20.68	−0.34	F16	19.36	0.93	S35	18.75	0.56
D48	17.82	1.07	F17	19.36	1.00	S36	18.68	0.18
D49	19.47	0.90	F19	20.77	−0.39	S37	18.29	0.80
D50	18.90	0.79	F20	19.05	0.88	S38	19.26	0.06
D51	19.25	0.71	F21	20.85	−0.34	S39	18.44	0.31
D52	19.53	0.82	F22	19.46	0.99	S40	18.65	0.04
D53	20.53	−0.44	F23	18.95	1.39	S41	16.57	0.62
D54	20.58	−0.04	F24	18.43	0.59	S42	17.24	0.73
D55	19.17	1.04	F27	19.22	0.48	S43	18.74	0.24
D57	20.44	0.48	F28	17.11	2.29	S44	18.78	0.35
D58	19.24	0.40	G2	20.60	−0.15	S45	18.72	0.64
D59	19.05	0.71	G3	18.94	0.82	S46	18.44	0.36
D60	19.36	0.77	G4	19.07	0.36	S47	19.00	0.49
D61	21.21	−0.10	G5	20.78	−0.21	S48	17.66	0.35
D62	21.55	0.04	G6	19.82	−0.05	S49	17.64	0.46
D63	19.32	1.11	G9	19.65	0.95	S50	18.18	0.37
D64	18.66	1.12	G10	18.38	1.23	S51	18.98	0.21
D65	18.64	1.28	G11	19.36	0.37	S52	17.55	0.67
D66	19.19	0.94	G12	18.04	1.20	S53	18.76	0.25
D67	21.18	0.75	G13	19.43	0.25	S54	18.77	0.12
D68	20.89	0.15	G14	18.40	0.82	S55	16.29	1.83
D69	20.73	0.87	G15	19.84	0.85	S56	18.47	0.77
D71	20.56	−0.12	G19	16.90	0.69	S57	18.38	0.37
D72	19.87	0.90	G20	19.13	1.13	S58	18.42	0.75
D73	20.47	0.82	G21	19.29	1.18	S59	17.22	0.84
D74	21.10	−0.40	H3	19.02	1.05	S61	18.92	0.68
D76	21.01	0.52	H4	20.66	0.14	S62	18.40	0.72
D77	20.94	0.00	H5	18.55	1.15	S64	18.65	0.38
D78	19.33	0.87	H6	17.15	1.44	S65	18.92	0.45
D80	17.78	1.36	H7	19.25	0.92	S66	18.03	0.84
D81	21.78	−0.29	H8	19.17	0.95	S67	18.22	0.56
D82	21.50	−0.41	H9	19.18	0.55	S68	19.28	0.31
D83	20.49	0.81	H12	19.99	0.01	S69	19.06	0.88
D84	21.47	−0.44	H13	19.33	0.15	S70	18.09	0.57
D85	21.85	0.06	H14	19.11	0.86	S72	18.94	0.67
D86	21.32	−0.36	H15	19.49	0.93	S75	19.29	0.88

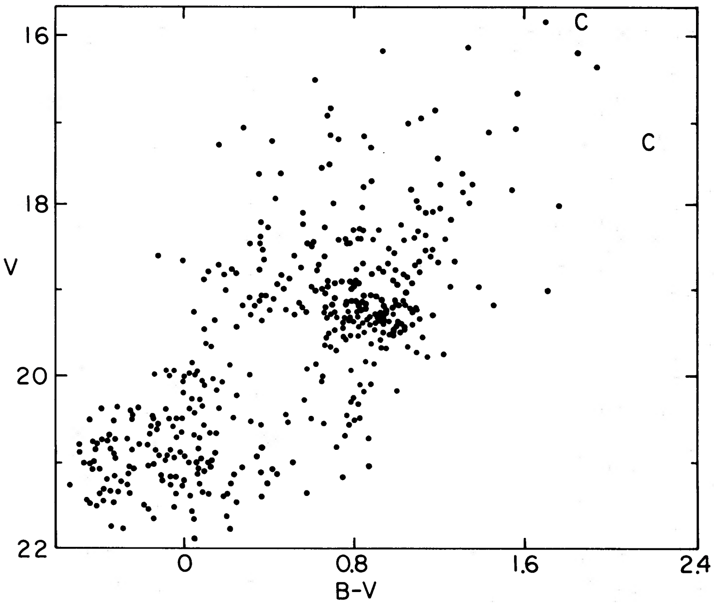

FIG. 2.—*C-M* diagram for all stars in NGC 152 for which even crude magnitudes could be measured. The carbon stars are indicated by C.

see Flower *et al.* 1980). This suggests that the clusters in the different parts of the Clouds might be thought of as condensations of the general stellar population. The field *C-M* diagram shows the main sequence reaching up to approximately $V = 21$ and a general concentration of giants in the color range $B-V \approx 1.0$ and at the level $V \approx 19.5$. The giant branch apparently extends up to $V \approx 17$ and $B-V = 1.6$ for the field stars. The fainter upper limit for the sparsely populated main sequence may indicate a generally older age for the field, though the number of stars is too small to make this a very strong statement. It is likely, instead, that the field has a range in age, with the majority of the stars having ages of one to a few billion years.

VI. THE CLUSTER COLOR-MAGNITUDE DIAGRAM

Figure 5 shows the color-magnitude diagram for NGC 152 that includes only those stars with V magnitudes that have a probable error of less than 0.7 mag. Several features of this diagram are significant. There is a well-populated main sequence at $B-V \approx 0.0$, extending from $V = 22$ up to $V = 20.0$. The main sequence width is large because of the uncertainties in the photometry below $V = 20$, leading to larger than average probable errors in the values of $B-V$ even for the select group of stars shown in this figure. The mean color of the main sequence agrees very well with the standard age-zero main sequence color for these absolute magnitudes, which in turn agrees with the fact that there is probably very little reddening in the SMC and in the foreground at this location (Sandage and Tammann 1974).

A second conspicuous feature of Figure 5 is a strong concentration of stars in a giant "clump" centered at $B-V = 0.95$ and $V = 19.3$. This group of giants is apparently identical to the so-called "clumps" of giants found in intermediate age clusters in our Galaxy (Cannon 1970), as well as in the Magellanic Clouds (Gascoigne 1980; Hodge 1980). It represents the stage of stellar evolution that occurs after giant branch evolution, when helium burning begins in the core and the star's temperature increases and its evolutionary progress slows down, leading to an accumulation of stars (Gascoigne *et al.* 1976). A comparison of the giant branch clumps in various clusters of the two Magellanic Clouds, including comparisons with stellar models and a semiempirical solution to the age and chemical composition problem, is given elsewhere (Hodge 1980).

A third feature of the color-magnitude diagram is the thinly populated giant branch extending from $B-V = 0.80$, $V = 20.5$, to $B-V \approx 2.0$ and $V = 16.5$. At the red tip of the giant branch there are two carbon stars (see § VIII).

A fourth feature of the color-magnitude diagram is a scattering of stars of intermediate color, most of them at $V \approx 17$ to 18 and ranging in color from $B-V = 0.2$ to the color of the giant branch. A comparison with the field color-magnitude diagram (§ V and below) shows that statistically the majority of these stars must be members of the cluster. All but one of the seven are located in the cluster core. We believe that these are most likely similar stars to those found in many other, somewhat younger, clusters in the Large Magellanic Cloud (LMC) (Flower and Hodge 1975; Flower *et al.* 1980). For reasons discussed in the latter of the above cited papers, it seems most likely that these are stars in an advanced stage of evolution, one which has not yet been predicted on theoretical grounds. A second possibility is that the stars represent an accumulation of multiple stars that for some dynamical reason are concentrated toward the center of this cluster. A discussion of these objects is presented in more detail elsewhere (Hodge 1981).

Figure 6 shows an alternative way of presenting the color-magnitude diagram of NGC 152, which allows the

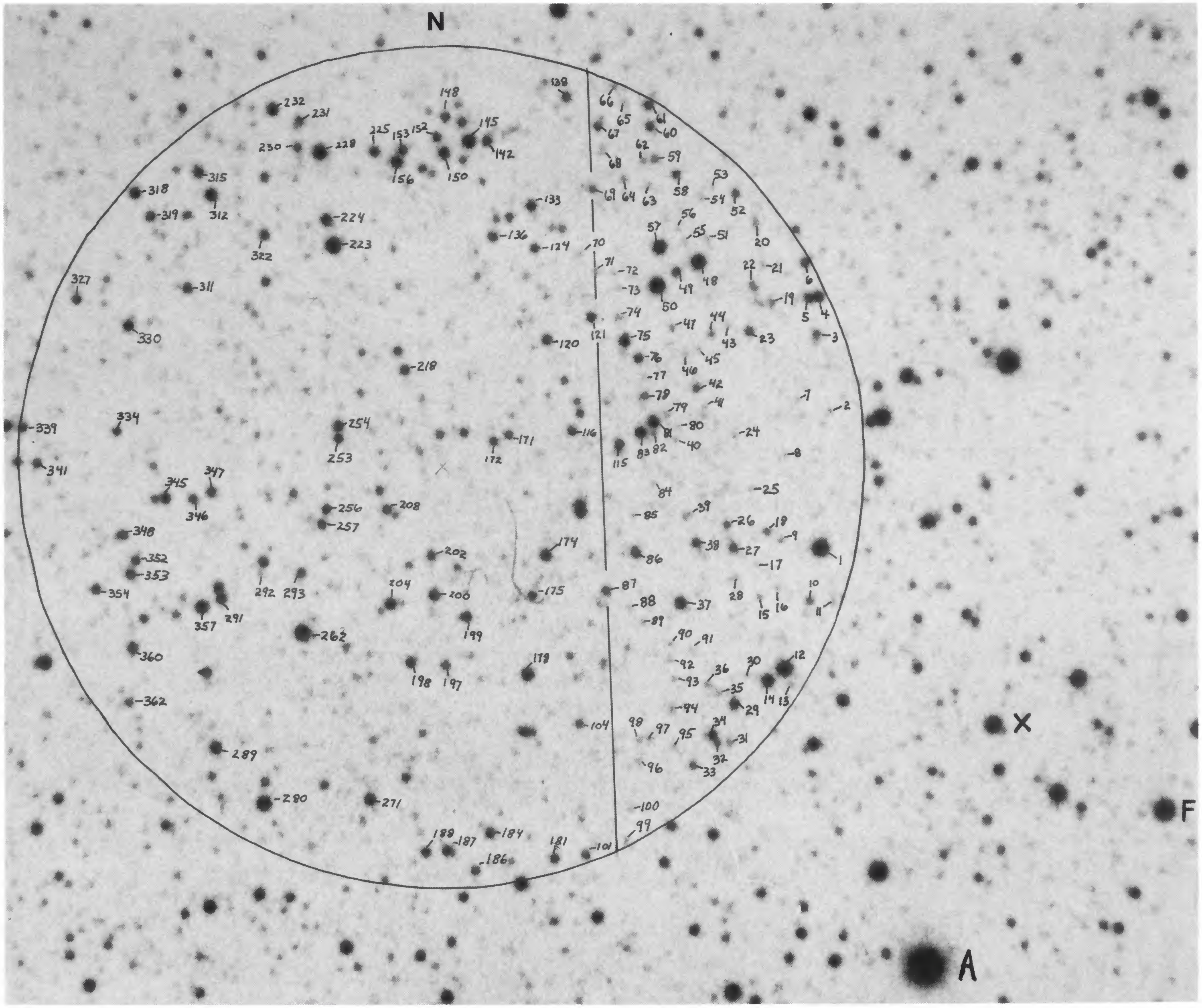

FIG. 3.—The SMC field near NGC 152 with measured field stars identified.

TABLE 4

FIELD STARS

Star	V	B-V	Star	V	B-V	Star	V	B-V	Star	V	B-V
1	17.19	1.11	45	22.07	0.37	89	21.96	-0.40	202	19.50	0.76
2	21.78	0.24	46	21.99	-0.51	90	22.05	0.49	204	18.57	1.06
3	19.86	0.57	47	21.25	0.39	91	22.46	-1.06	208	19.32	0.78
4	18.58	0.40	48	17.86	1.18	92	22.11	-0.38	218	19.40	0.81
5	19.25	0.74	49	19.59	0.84	93	22.10	-0.15	223	17.48	1.37
6	19.32	0.52	50	17.39	1.69	94	21.01	-0.25	224	18.82	0.83
7	22.14	-0.91	51	22.04	0.13	95	21.76	-0.63	225	19.29	0.91
8	22.33	-0.58	52	19.86	0.59	96	21.78	-0.35	228	17.85	1.13
9	21.45	0.26	53	22.72	-1.39	97	21.29	0.25	230	19.57	0.96
10	20.07	0.60	54	21.93	-0.42	98	21.40	0.03	231	19.51	0.48
11	21.75	-0.95	55	22.05	-0.57	99	22.04	-0.96	232	18.61	1.05
12	17.37	1.65	56	22.40	-0.99	100	22.74	-0.68	253	19.09	1.22
13	21.10	-0.13	57	18.16	1.04	101	19.80	0.82	254	18.96	1.02
14	18.25	1.34	58	19.74	0.59	104	19.78	0.59	256	19.32	1.25
15	21.57	-0.55	59	20.13	0.03	115	19.20	0.44	257	19.31	0.85
16	22.34	-0.32	60	19.53	0.89	116	19.48	1.01	262	17.54	1.22
17	22.51	-0.20	61	19.35	1.07	120	19.23	0.88	271	18.66	1.11
18	20.21	0.22	62	21.19	-0.30	121	19.39	1.07	280	17.74	1.79
19	20.31	0.38	63	21.83	-0.46	124	19.67	0.88	289	18.54	0.01
20	20.70	0.26	64	21.29	0.01	133	19.19	0.90	291	18.88	1.05
21	22.07	-0.62	65	22.05	-0.94	136	19.44	0.76	292	19.02	1.00
22	20.23	0.24	66	20.95	0.00	138	19.54	0.71	293	19.55	0.39
23	19.64	0.55	67	19.90	0.45	142	19.10	0.97	311	19.13	0.90
24	22.20	-0.64	68	21.61	-0.18	145	18.20	1.28	312	18.61	1.20
25	22.71	0.24	69	19.99	0.73	146	19.44	0.71	315	18.88	0.69
26	20.14	0.71	70	22.04	-0.75	148	19.49	0.99	318	18.89	1.23
27	19.46	0.51	71	22.05	-0.70	150	18.70	0.73	319	19.26	1.21
28	22.01	-0.69	72	22.16	-0.41	152	19.51	0.90	322	19.22	0.81
29	19.15	0.68	73	22.46	-0.35	153	19.13	-0.83	327	19.32	0.86
30	22.30	-0.36	74	21.28	-0.47	156	18.27	0.96	330	18.88	0.98
31	20.46	0.24	75	18.71	0.88	171	19.58	0.14	334	19.78	0.99
32	19.83	1.08	76	19.51	0.83	172	19.67	0.93	339	19.18	0.58
33	20.09	0.22	77	22.74	-0.68	174	18.79	1.16	341	19.45	1.13
34	19.07	0.86	78	19.91	0.51	175	19.52	0.56	345	18.93	1.03
35	21.36	-0.66	79	21.16	-0.10	178	18.53	1.00	346	19.46	0.87
36	21.25	0.00	80	22.37	-0.40	181	19.60	0.96	347	19.27	0.93
37	18.57	0.85	81	18.46	0.88	184	19.21	0.68	348	19.11	0.68
38	19.45	0.12	82	20.05	0.86	186	19.65	0.96	352	19.25	0.38
39	20.84	-0.20	83	18.67	0.64	187	18.99	0.66	353	18.92	0.64
40	22.05	-0.13	84	22.55	-0.91	188	19.46	1.08	354	19.26	0.86
41	22.24	-1.16	85	22.74	0.14	197	19.59	0.83	357	18.29	1.25
42	19.96	0.16	86	19.05	0.77	198	19.23	1.02	360	18.94	0.86
43	22.22	-0.36	87	19.61	0.97	199	19.04	1.38	362	19.75	0.01
44	20.55	0.72	88	22.19	-0.48	200	18.91	1.24			

reader to gauge the effects of contamination of the diagram by field stars. In this figure we compare the number of stars in the NGC 152 *C-M* diagram for each square of the array with the number of stars in that color-magnitude interval found in the field diagram. In the case of the field diagram numbers, statistical corrections have been made to allow for the difference in the area covered and for the difference at different magnitude levels of the loss of plotted stars in NGC 152 due to crowding. The result shows that most of the main sequence stars and giant stars are members of NGC 152, while the field stars occupy primarily regions of intermediate color (particularly around $V = 20$). Figure 7 is a third representation of these data, in which a statistical subtraction of stars in the color-magnitude diagram has been effected by using the field diagram (corrected for equivalent coverage at different magnitudes) to remove stars from the cluster diagram. In this case, the cluster diagram stars nearest in plotted position to equivalent stars in the field diagram were removed, giving a cleaned diagram of cluster stars only.

VII. INTERPRETATION OF THE COLOR-MAGNITUDE DIAGRAM

In the following discussion I am using the distance modulus, reddening, and absorption for the Small Magellanic Cloud that was derived by Sandage and Tammann (1974). Conclusions regarding the age and chemical composition of NGC 152 would be somewhat altered if instead the distance modulus and reddening proposed by de Vaucouleurs (1978) were used. It should be noted that the latter does not seem to fit the observations of the main sequence as well as the Sandage-Tammann distance and reddening, as is illustrated in Figure 8, which shows a comparison of the observations with the Yale isochrones (Ciardullo and Demarque 1977) for stars with $Z = 0.007$ and $A = 2 \times 10^9$ yr, the lower age limit suggested for this cluster by Mould and Aaronson (1980) on the basis of its

1981ApJ...247..894H

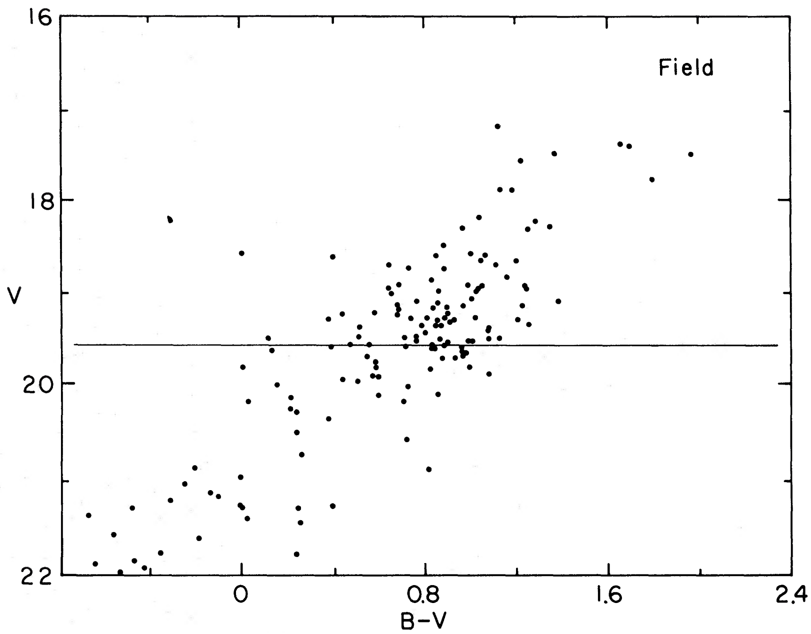

FIG. 4.—The *C-M* diagram for the field near NGC 152. See text for a discussion of completeness to different magnitude limits.

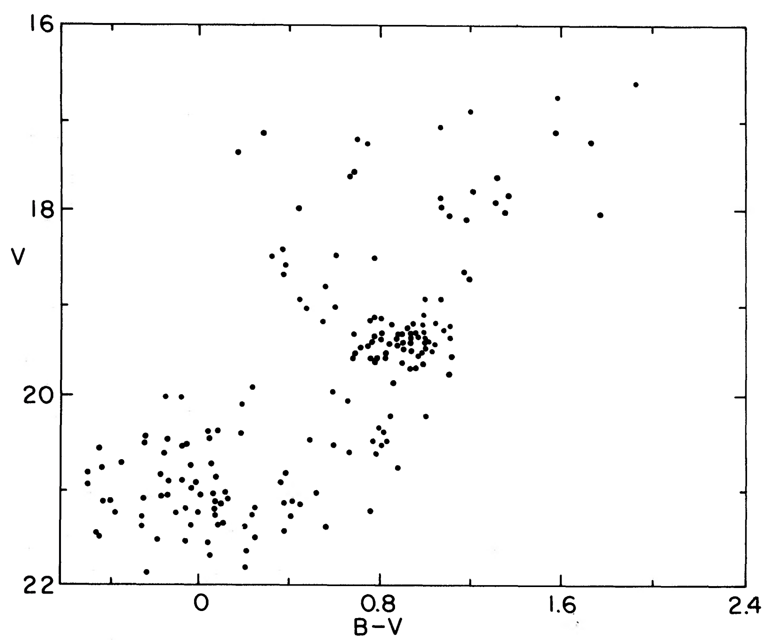

FIG. 5.—The *C-M* diagram for NGC 152, including only those stars for which the probable error in *V* is less than 0.07.

1981ApJ...247..894H

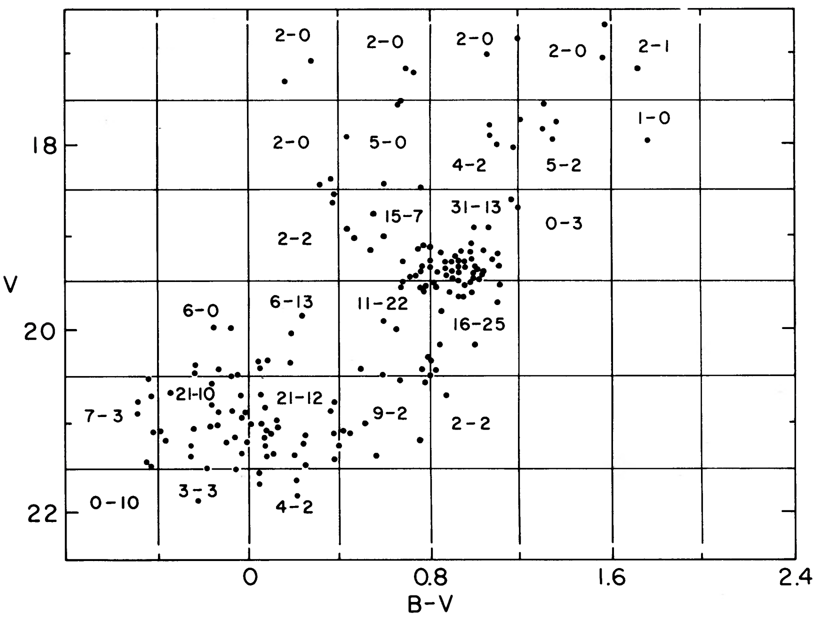

FIG. 6.—A comparison of the NGC 152 *C-M* diagram (*points* and *left-hand* numbers in each box) with the field (*right-hand* numbers), all corrected for relative completeness.

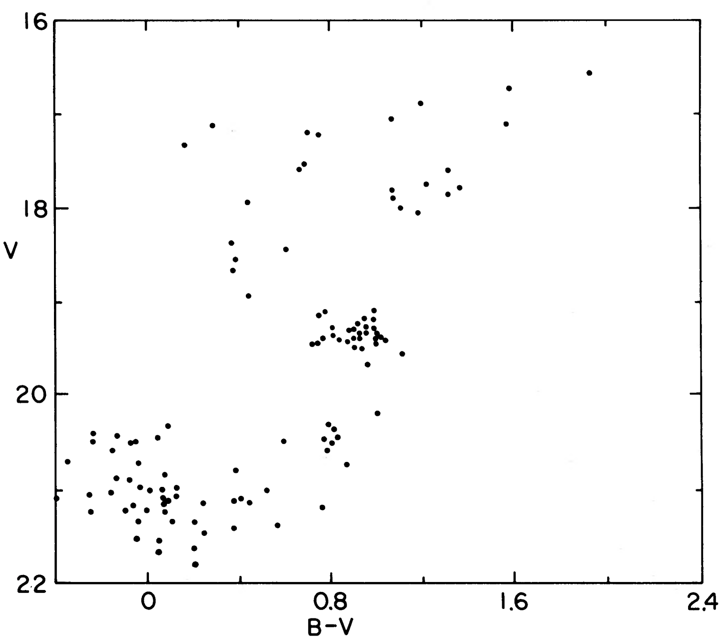

FIG. 7.—The NGC 152 *C-M* diagram from which field stars have been removed statistically.

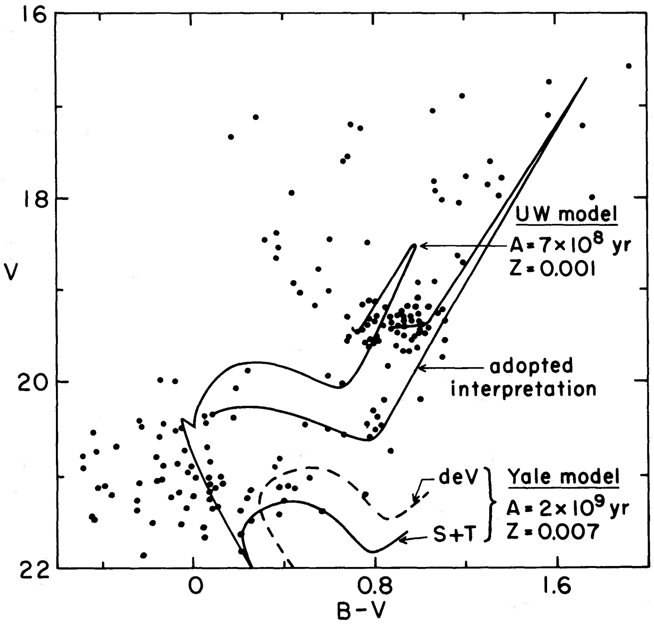

FIG. 8.—A comparison of the NGC 152 *C-M* diagram with a Yale isochrone for $Z = 0.007$ and $A = 2 \times 10^9$ yr, assuming two different assumptions about reddening and distance. Also shown is a model calculated by Flower *et al.* (1980) and an adopted *C-M* diagram interpretation.

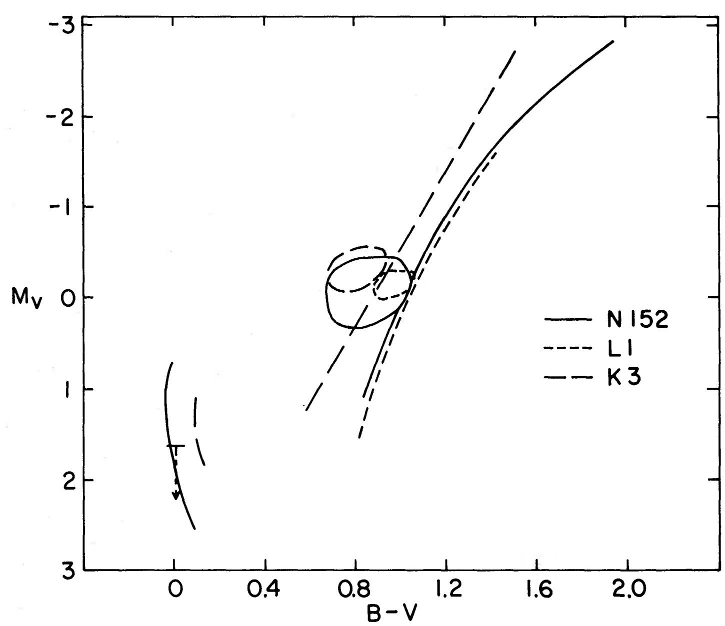

FIG. 9.—A comparison of schematic *C-M* diagrams for three SMC clusters for which faint photometry is available

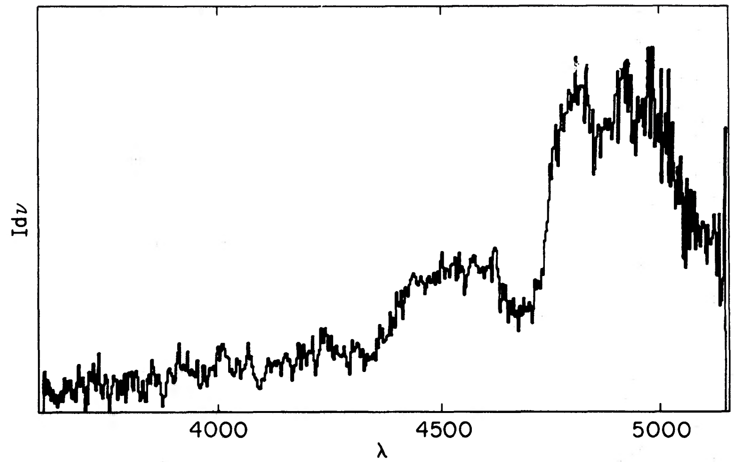

FIG. 10.—The spectrum of the carbon star H23, obtained with the RC spectrograph and the SIT-Vidicon on the CTIO 4 m telescope.

integrated colors. This comparison also shows that these particular values of the Yale isochrones are inappropriate for NGC 152 no matter which distance modulus and reddening is assumed, the cluster being considerably younger than 2 billion years if the composition is anything like that of the Yale model.

Figure 9 shows a comparison of NGC 152 with two other SMC clusters for which photometry is available to similar magnitude limits, Lindsay 1 and Kron 3 (Gascoigne 1980). It is clear that SMC clusters are fairly similar in the main properties of their color-magnitude diagrams. NGC 152 seems to be the youngest of the three, with a main sequence turn off point that is approximately half a magnitude brighter than for Kron 3 (although this is somewhat uncertain because of poor statistics of stars on the upper main sequence) and more than a magnitude brighter than the main sequence turnoff for Lindsay 1. The giant branch of NGC 152 is very similar in color to that for Lindsay 1, except for the fact that it extends to brighter and redder limits. It is significantly redder than that for Kron 3, a fact which is most likely accounted for by a difference in the chemical abundances for the two clusters. The magnitude for the clump of stars in the giant region, which we identify as the equivalent of blue loops in younger clusters or the horizontal branch in older clusters, is approximately the same for the three clusters, $M_V = 0.0 \pm 0.5$.

A more complete discussion of the color-magnitude diagram's interpretation in terms of both age and chemical abundances is given elsewhere (Hodge 1980). There an array of observationally calibrated theoretical *C-M* diagram parameters leads to a value of $Z = 0.0035$ and an age of 8×10^8 yr for NGC 152. It is thus similar in age to NGC 1868 in the LMC (Flower *et al.* 1980), but is less metals-poor. NGC 1868's slightly younger age and its very blue giant branch both account for the cluster's bluer integrated color ($B - V = +0.45$, as compared to $+0.70$ for NGC 152).[2]

TABLE 5

CARBON STARS AND VERY RED STARS

Star Name	V	$B - V$	Type[a]
Confirmed carbon stars:			
H23	15.98[b]	1.66	C,2
F28	17.11	2.29	C,4
Very red stars:			
B11	16.52	1.93	K5
C19	15.88	1.71	M0
E18	16.70	1.58	K5
S5	16.84	3.17	...
S55	16.29	1.83	...

[a] From Mould and Aaronson 1980.
[b] Variable.

VIII. THE CARBON STARS

Star H32, one of the brightest in the cluster, was examined with the Cassegrain Spectrograph and the SIT Vidicon on the CTIO 4 m telescope on 1979 September 27. Grating 26, giving a dispersion of 100 Å mm^{-1} over 3600–5200 Å, was used with a 600 μm slit width. Standard CTIO 10th mag stars were used for the reductions, which were carried out on the La Serena computer. The star turned out to be very red (Table 5), and its spectrum (Fig. 10) is that of a carbon star. Mould and Aaronson (1980) independently identified this object as a carbon star, classifying it as type C,2. Additionally, they found star F28 to be a carbon star of type C,4. We have picked out other red stars and likely candidates, based on their locations in the *C-M* diagram.

I wish to acknowledge the help of Richard Dickson who did the astrophotometry, Edward Olszewski who

[2] After this paper was written, N. J. Stewart kindly sent me a portion of his Ph.D. thesis, which includes data on NGC 152, for which he derives a similar age.

reduced the photoelectric measures, and Hugh Harris who reduced the spectrophotometry. I am also indebted to Phillip Flower for many helpful discussions and for letting me use some of his plates of NGC 176, which had images of NGC 152 on them. Most of this research was carried out with financial support from the National Science Foundation under grants AST-76-17598 and AST-7915148.

REFERENCES

Alcaino, G. 1978, *Astr. Ap. Suppl.*, **34**, 431.
Baird, S., Flower, P., Hodge, P., and Szkody, P. 1974, *A.J.*, **79**, 1365.
Cannon, R. 1970, *M.N.R.A.S.*, **150**, 111.
Ciardullo, R., and Demarque, P. 1977, *Trans. Astr. Obs. Yale Univ.*, Vol. **33**.
de Vaucouleurs, G. 1978, *Ap. J.*, **223**, 730.
Flower, P. 1976, Ph.D. thesis, University of Washington.
Flower, P., Geisler, D., Hodge, P., and Olszewski, E. 1980, *Ap. J.*, **235**, 769.
Flower, P., and Hodge, P. 1975, *Ap. J.*, **196**, 369.
Gascoigne, S. 1980, in *IAU Symposium 85, Star Clusters*, ed. J. Hesser (Dordrecht: Reidel), p. 305.
Gascoigne, S., and Kron, G. 1952, *Pub. A.S.P.*, **64**, 196.
Gascoigne, S., Norris, J., Bessell, M., Hyland, A., Visvanathan, N. 1976, *Ap. J. (Letters)*, **209**, L25.
Hesser, J., Hartwick, F., and Ugarte, P. 1976, *Ap. J. Suppl.*, **32**, 283.
Hodge, P. 1960, *Ap. J.*, **131**, 351.
———. 1963, *Ap. J.*, **137**, 1033.
———. 1980, preprint.
———. 1981, *Astr. Ap.*, in press.
Mould, J., and Aaronson, M. 1980, *Ap. J.*, **240**, 464.
Pickering, E. 1891, *Ann. Harvard Obs.*, **27**, 14.
Racine, R. 1969, *Ap. J.*, **74**, 1073.
Sandage, A. R., and Tammann, G. 1974, *Ap. J.*, **190**, 525.
Searle, L., Wilkinson, A., and Bagnuolo, W. 1980, preprint.
van den Bergh, S., and Hagen, G. 1968, *A.J.*, **73**, 569.
Walker, M. 1971, *Ap. J.*, **167**, 1.
———. 1979, *M.N.R.A.S.*, **186**, 767.

P. W. HODGE: Astronomy Department, FM-20, University of Washington, Seattle, WA 98195